JOURNAL OF AIRCRAFT
Vol. 31, No. 5, Sept.–Oct. 1994

Influence of Structural and Aerodynamic Modeling on Flutter Analysis

Alfred G. Striz*
University of Oklahoma, Norman, Oklahoma 73019
and
Vipperla B. Venkayya†
Wright Laboratories, Wright-Patterson Air Force Base, Ohio 45433

The dynamic aeroelastic capabilities in the automated structural optimization system were used to evaluate the flutter behavior of various fully built-up finite element wing models in subsonic and supersonic flow. First, the performance of the flutter module was tested against results from other codes. Then, models of various wings with different aspect ratios were investigated for the influence on the free vibration and flutter characteristics of such modeling factors as finite element selection, structural grid refinement, number of selected modes, retention of in-plane and breathing modes, aerodynamic panel size and placement, splining of the aerodynamic grid to the structural grid, selection of extra points off the structural wing box for splining, solution procedures such as eigenvalue extraction routines, reduction schemes, etc. The results suggest that a quick initial evaluation of a preliminary wing design with a reasonably coarse grid for both the structure and the aerodynamics will result in natural frequencies and modes that are close to those from a more detailed model and in flutter speeds that tend to be conservative. Overall, such a simple model can represent a good start for a conventional redesign process as well as for optimization.

Introduction

IN recent years, structural optimization as needed and used by the aerospace industry has expanded in scope to include such additional disciplines as static and dynamic aeroelasticity, composite materials, aeroelastic tailoring, etc. One of the more promising multidisciplinary codes presently under development is the automated structural optimization system (ASTROS).[1–3] In this computer code, static, dynamic, and frequency response finite element structural modules, subsonic and supersonic steady and unsteady aerodynamic modules, and an optimization module are combined and allow for either analysis or optimized design of given aircraft configurations. Interfering surface aerodynamics are incorporated to handle the aerodynamic modeling of combinations of wings, tails, canards, fuselages, and stores. Structures are represented by fully built-up finite element models, constructed from rod, membrane, shear, plate, and other elements. Static and dynamic aeroelastic capabilities include trim, lift effectiveness, aileron effectiveness, gust response, and flutter analysis.

In this article, as part of an ongoing effort to gain a better understanding of the optimization process with aeroelastic constraints, the flutter analysis portion of ASTROS was used for various investigations of fully built-up finite element wing models in subsonic and supersonic flow to determine the influences of structural and aerodynamic modeling on flutter analysis and, thus, to investigate the behavior of the analyses modules of the code. This knowledge is incidental to the understanding of the dynamic behavior of wings during the optimization process. It will also result in better initial models and, thus, a more efficient optimization cycle.

First, the performance of the flutter analysis module was evaluated against results by other methods and codes such as the large-scale finite element code MSC/NASTRAN[4] and the flutter analysis code FASTEX.[5] Similar comparisons for beam-type wing models were performed by Garner and French[6] and by Pendleton et al.[7] with good results. Here, the wing (Fig. 1), used by Rudisill and Bhatia,[8,9] McIntosh and Ashley,[10] Segenreich and McIntosh,[11] and others for structural optimization with flutter constraints, was chosen since it represents one of the few models where all structural, material, and environmental data are given for aeroelastic analysis.

It is well known that the normal modes response depends on the structural modeling and the nonstructural mass distribution only, whereas flutter and optimization results depend on and vary with the quality of the structural modeling, the aerodynamic modeling, and the splining connecting the structural and the aerodynamic representations. Thus, the main interest of this investigation was to determine the influences of the structural models, the aerodynamic models, and the splining on the free vibration frequencies and mode shapes, and the flutter speeds.

For this investigation, the simple rectangular unswept wing shown in Fig. 1 was used for the initial comparison. In ad-

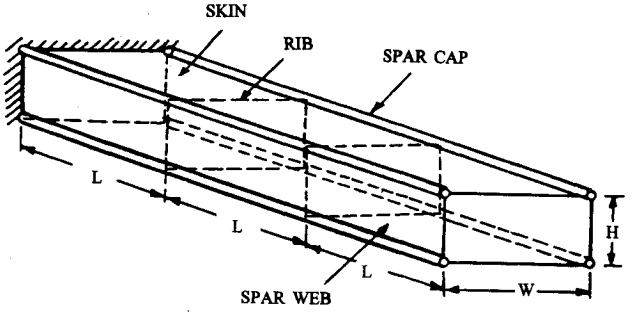

Fig. 1 Wing model of Ref. 8.

Presented as Paper 90-0954 at the AIAA/ASME/ASCE/AHS/ASC 31st Structures, Structural Dynamics, and Materials Conference, Long Beach, CA, April 2–4, 1990; received July 20, 1992; revision received Feb. 11, 1994; accepted for publication Feb. 11, 1994.

*Associate Professor, Aerospace and Mechanical Engineering. Associate Fellow AIAA.

†Principal Scientist, Flight Dynamics Laboratory. Associate Fellow AIAA.

Table 1 Varying element types on wing model of Ref. 8

Ribs:	Membrane elements	Shear elements	Membrane elements
Spars:	Membrane elements	Membrane elements	Shear elements
		Natural frequency, Hz	
	10.50 B	10.50 B	6.26 B
	26.60 T	26.60 T	24.75 T
	55.86 B	55.85 B	37.57 B
	79.12 T	79.12 T	71.77 T
	125.83 B	125.81 B	110.35 B
	134.42 T	134.42 T	122.65 T
		Flutter speed, in./s	
	10,881	10,881	10,400

B = bending, T = torsion.

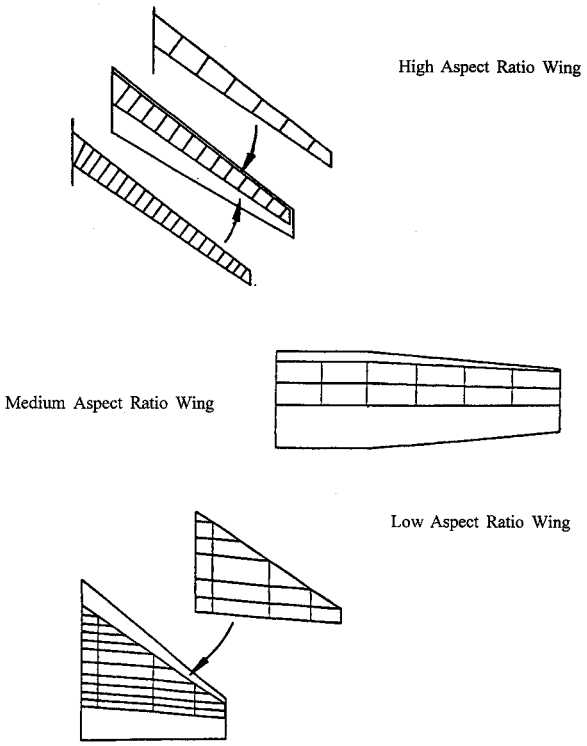

Fig. 2 Wing planforms used for modeling in flutter analysis.

dition, a set of test cases was selected consisting of a high aspect ratio swept and tapered wing, a medium aspect ratio straight wing with a tapered section toward the wingtip, and a low aspect ratio swept and tapered fighter-type wing (Fig. 2). The straight wing and the high aspect ratio wing were evaluated at subsonic Mach numbers, whereas the fighter wing was investigated for flutter at subsonic and supersonic speeds. All wings were cantilevered and fixed at the root.

Background

The importance of this investigation can be seen from the following example: It is generally understood that membrane elements when used for spars and ribs overpredict the stiffness of a wing. Thus, when the wing used by Rudisill and Bhatia was modeled by the present authors by replacing the front and rear spar membrane elements with shear elements, the natural frequencies of the first three bending modes dropped from 10.5, 55.9, and 125.8 Hz to 6.3, 37.6, and 110.3 Hz, respectively. This kind of change in wing bending frequencies can have a considerable impact on control surface performance and flutter. However, this example represents only a structural modeling change. In a flutter analysis, the aerodynamic modeling can have similar effects on the results: the number, size, and distribution of the aerodynamic panels and

Table 2 Varying aerodynamic paneling schemes on modified wing model of Ref. 8

Spanwise:	6	6	15	15	24	24
Chordwise:	4	9	4	9	4	9
			Flutter speed, in./s			
	9,945	9,992	10,267	10,314	10,348	10,400

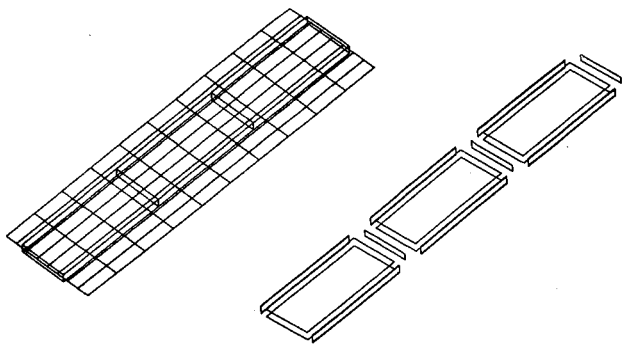

Fig. 3 Exploded view of wing in Ref. 8.

the splining between the aerodynamic points and the structural grid can influence the flutter speed and the flutter mode shapes. In ASTROS, a surface spline is used for the aerodynamic force transfer to the wing structure while a cubic spline is incorporated to compute the matrix of aerodynamic coefficients, Mach numbers, and reduced frequencies for the pk-flutter analysis, with additional splining options available in the latest releases of the code.

Any optimization is only as good as the associated analyses, and, in some cases, can compound and exaggerate errors arising from them. Thus, if modeling errors can have a considerable impact on the quality of the results of the associated analyses, an optimization can be seriously jeopardized to the point where the resulting optimal design can be not only wrong, but dangerous. In the above example, use of the stiffer membrane elements resulted in a 10% lower minimum weight design (38.03 lb), as compared to the more realistic, less stiff shear elements (42.5 lb). If the flutter constraint is the driving constraint, this could lead to the design of a structure that is potentially too weak. It is, therefore, essential that the initial designs used in optimization are feasible and modeled correctly, especially when fully built-up finite element structural models are used rather than the previously more common beam models.

Thus, fully built-up finite element structural models for the four wings were evaluated for flutter behavior and the influence of such modeling factors as finite element selection, structural grid refinement; number of selected modes, retention of in-plane and breathing modes; aerodynamic panel size and placement; splining of the aerodynamic grid to the structural grid; the selection of extra points off the structural wing

Table 3 Geometrical, material, and environmental property model data

	High aspect ratio wing (transport/bomber type wing) $M = 0.60$, $h = 5{,}000$ ft; $M = 0.87$, $h = 30{,}000$ ft	
Variation:	7 ribs, 14 ribs, 21 ribs	
Input[a]:	Shear panel thickness:	0.15–0.10 in. in ribs (for 14-rib) 0.20–0.10 in. in spars
	Membrane thickness:	0.30–0.10 in. in skins
	Spar cap cross-sectional area:	3.6–3.0 in.^{2}
	Spar stiffener cross-sectional area:	0.20 in.^{2}
	Medium aspect ratio wing (light transport/combat aircraft type wing) $M = 0.58$, $h = 5{,}000$ ft	
Variation:	No MPCs, aerodynamic MPCs (14 points), mass MPCs (14 points); number of aerodynamic boxes; splining overlap	
Input:	Shear panel thickness:	0.08 in. in spars and ribs
	Membrane thickness:	0.06 in. in skins
	Spar cap cross-sectional area:	1.0 in.^{2}
	Spar stiffener cross-sectional area:	0.2 in.^{2}
	Low aspect ratio wing (fighter type wing) $M = 0.5$, $h = 5{,}000$ ft	
Variation:	5 spars, 10 spars; input Mach number	
Input[a]:	Shear panel thickness:	
	0.08 in. in ribs	
	0.15–0.06 in. in spars (5-spar)	
	0.075–0.03 in. in spars (10-spar)	
	Membrane thickness:	0.25–0.04 in. in skins
	Spar cap cross-sectional area:	2.0–1.0 in.^{2} (5-spar)
		1.0–0.5 in.^{2} (10-spar)
	Spar stiffener cross-sectional area:	0.05 in.^{2}
Material:	$E = 1.0 \times$ E7 lb/in.^{2}, $\nu = 0.33$, $\rho = 0.1$ lb/in.^{3}	

[a]All values decreasing from root to tip.

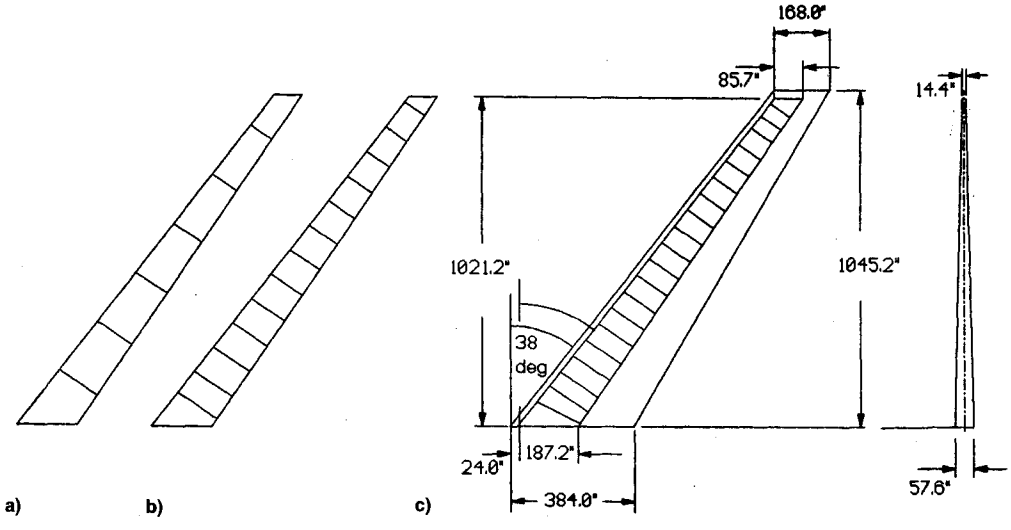

Fig. 4 High aspect ratio wing with a) 7, b) 14, and c) 21 ribs.

box (multipoint constraints or MPCs) for better mass distribution and aerodynamic splining; solution procedures such as reduction schemes, etc., and results are presented.

Rudisill and Bhatia Wing Model

The finite element wing model used by Rudisill and Bhatia and later by other researchers (shown in an exploded view in Fig. 3) represents one of the very few cases in the flutter optimization literature where all structural, material, and environmental data were given to allow for a direct comparison of results. It was, therefore, chosen in the present study for this same purpose.

However, three drawbacks of the model have to be pointed out:

1) The aspect ratio of the spar web elements in the model is 15, thus, too high for a reliable performance of the element, even in dynamic analysis.

2) The spar webs are modeled by membrane elements rather than shear elements, which results in an unrealistically stiff structure.

3) Since no nonstructural distributed mass was added to the model, the mass center of the wing coincides with the elastic axis, resulting in a close proximity of flutter speed and divergence speed as first suggested by Eastep.[11]

Here, for the base model with skins, ribs, and webs all modeled by membrane elements, the flutter speed for an input Mach number of $M = 0.5566$ and an altitude of $h = 10{,}000$ ft was calculated by ASTROS and MSC/NASTRAN as 10,881 and 10,500 in./s, respectively, with divergence speeds of 11,900 and 11,500 in./s, respectively. It has to be pointed out that MSC/NASTRAN no longer supports pure membrane elements, but uses QUAD4 elements instead. The flutter analysis code FASTEX computed a flutter speed of 10,525 in./s, based on the ASTROS mode shapes, but did not show a

divergence branch in the root-locus plot. The flutter speed shown in Fig. 3 of Ref. 8 for the initial configuration was about 10,800 in./s. When the optimized versions of the model as obtained in Refs. 10 and 11 were analyzed for flutter, they were found to all encounter a divergence speed much lower than the speed used as a flutter constraint. It seems that none of these optimizations included the possibility of divergence as a flutter root with zero frequency. Thus, the size distributions of these optimized results seem to have been limited to flutter constraints only and would have resulted in designed wing models that considerably exceeded their divergence speeds.

First, in order to test the influence of the finite element selection on the natural frequencies, the mode shapes, and the flutter speed, the spar webs as well as the ribs were alternately modeled as shear elements and as membrane elements. The rest of the model was kept as in Ref. 8. All not out-of-plane displacements were eliminated by Guyan reduction and aerodynamic MPCs were used. The results are presented in Table 1.

It can be seen that changing the ribs from membrane elements to shear elements did not seem to influence the natural frequencies at all, nor did it have any impact on the flutter speed. However, when the spar webs were changed from membranes to the more realistic shear elements, there was a significant drop in the first three bending frequencies (40, 33, and 12%, respectively), whereas the first three torsion frequencies dropped by only about 8% each. At the same time, the flutter speed dropped by about 5%, indicating that the all-membrane model was nonconservative. Then, to examine the influence of the number of aerodynamic boxes on the wing, various paneling schemes were chosen for the model with shear elements for spar webs: 6 spanwise × 4 chordwise, 6 × 9, 15 × 4, 15 × 9, 24 × 4, and 24 × 9. Results are presented in Table 2.

Here, the results for the cases with coarse (6 × 4 and 6 × 9) spanwise mesh distribution were almost identical (0.5%), as were those of the medium (15 × 4 and 15 × 9, difference 0.5%) and fine (24 × 4 and 24 × 9, difference 0.5%) spanwise distributions. Quadrupling the spanwise distribution increased the flutter speed somewhat (4%). These results seem to indicate that a reasonably coarse mesh, used to save computer time for quick preliminary analyses, can at least result in a conservative approximation to the flutter speed.

Varying the input Mach number from $M = 0.5566$ to 0.65 and, finally, to 0.717 for the all-membrane wing model with a 24 × 9 aerodynamic mesh, increased the flutter speed very slightly, from 10,881 to 10,943 to 11,010 in./s, respectively. Then, a decrease in altitude from $h = 10{,}000$ ft at $M = 0.717$ to $h = 4500$ ft (initial conditions from Ref. 12) lowered the flutter speed as expected, in this case to 10,320 in./s.

Finally, the free vibration mode shapes computed for the base wing model showed a considerable number of in-plane, breathing, and stretching modes. It was considered advantageous to eliminate these from the flutter calculations to improve convergence and to omit false flutter points that occurred when the solution algorithm jumped between modes, especially for the case of included in-plane modes. From the obtained results, it became clear, however, that only the in-plane modes need to be eliminated, which is most easily done by Guyan reduction to only out-of-plane displacements. Omitting those breathing and stretching modes that had mostly out-of-plane displacements, in addition to the in-plane modes, did not seem to change the flutter results by a noticeable amount. Almost identical results were obtained with MSC/NASTRAN.

Three Wing Models with Different Aspect Ratios

The three wing models selected represent, in order, 1) a swept and tapered transport/bomber type wing of high aspect ratio, 2) a straight and partially tapered light transport/combat aircraft type wing of medium aspect ratio, and 3) a swept and tapered fighter type wing of low aspect ratio.

As pointed out earlier, a severe deficiency in many flutter analysis reports is the absence of adequate details with respect to the structural and aerodynamic modeling to allow for a meaningful comparison with results obtained by other methods. Thus, for all structural and aerodynamic models used in the present investigation, all necessary dimensions as well as parameters are available in a report[13] to allow for such comparisons. Some selected structural and environmental data for these wings are given in Table 3.

The structural models for the three wings were built up from rod, membrane, and shear elements to represent the wing boxes with spars, spar caps, spar stiffeners, ribs, and skins. Here, the rods corresponded to spar caps and spar stiffeners, the membranes were used for the skins, and the shear elements for the spar webs and ribs of the wings. All three wings were cantilevered and fixed at the root.

Table 4 Varying rib number on high aspect ratio wing model

Number of ribs		
7	14	21
Natural frequency, Hz		
1.09 B	1.08 B	1.09 B
4.04 B/T	3.99 B/T	4.05 B/T
8.67 T	8.74 T	8.76 T
9.48 T/B	9.29 T/B	9.37 T/B
15.24 T/B	15.43 T/B	15.51 T/B
16.73 T/B	16.45 T/B	16.47 T/B
Flutter speed, in./s		
[$M = 0.60$] 14,607	14,721	14,972
[$M = 0.87$] 20,756	20,719	20,938

B = bending, T = torsion.

Table 5 Varying number of aerodynamic panels on medium aspect ratio wing model

Panel mesh					
5 × 5	5 × 10	11 × 5	11 × 10	22 × 5	22 × 10
Flutter speed, in./s					
19,512	19,581	19,912	19,969	20,167	20,240

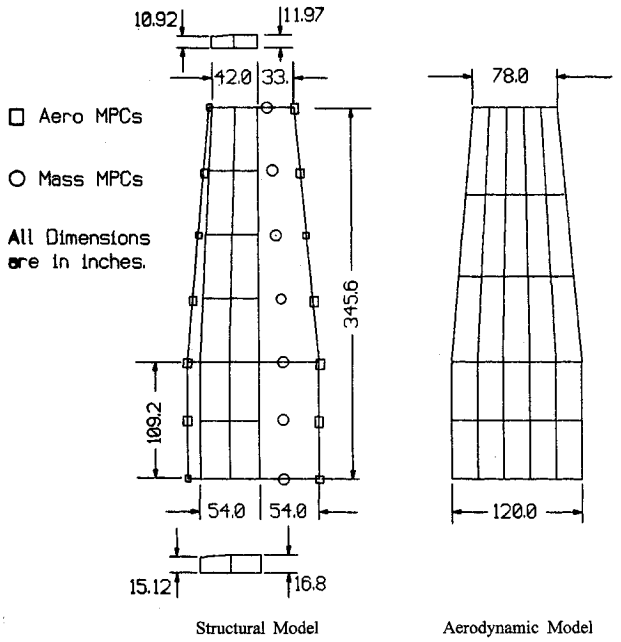

Fig. 5 Medium aspect ratio wing with all MPCs.

Table 6 Use of multipoint constraints on medium aspect ratio wing model

Without MPCs	Aero MPCs	Mass MPCs	Both MPC sets
		Natural frequency, Hz	
3.22 B		3.22 B	
16.40 B/T		16.31 B	
20.14 T		18.72 T	
41.16 T		40.43 B/T	
48.35 T		45.01 T	
73.13 Br		8.91 T	
		Flutter speed in./s	
15,563 (16.6 Hz, low g)		12,239 (16.5 Hz, hump mode)	
22,779 (7.3 Hz)	21,395 (7.4 Hz)	21,156 (7.3 Hz)	20,238 (7.4 Hz)
24,220 divergence			

B = bending, T = torsion, Br = breathing.

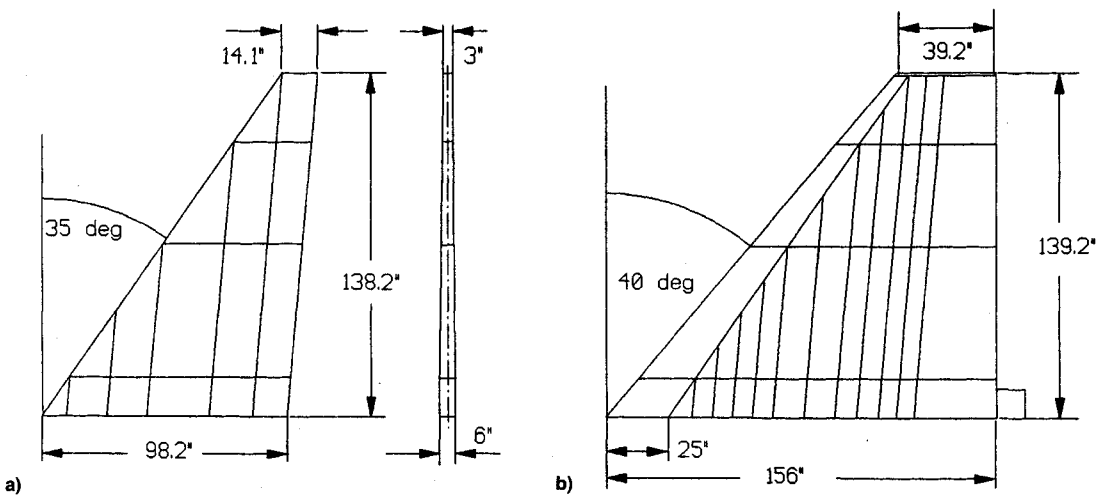

Fig. 6 Low aspect ratio wing with a) 5 and b) 10 internal spars.

High Aspect Ratio Wing

For the high aspect ratio wing, the structural weight was assumed to be 30% of the overall weight of the wing, with the other 70% distributed as nonstructural masses at all nodal points. No MPCs were used. For the flutter analyses, Guyan reduction was applied to retain out-of-plane displacements only.

For this wing, the influence of structural complexity in spanwise direction was evaluated. The original wing model consisted of a reasonable box with 14 bays, showing good aspect ratios in most of the elements. Then, the wing was modeled in a simpler form with only 7 bays and also subdivided into a larger number of bays (21) while keeping the total weight constant. The reasonable width-to-length ratio of the elements was herein exceeded, especially in the seven-bay model to determine how forgiving the structural modeling process is (Figs. 4a, 4b, 4c, and Table 4).

From these results, it seems that a spanwise increase in the complexity of the structural modeling has very little, if any, influence on the natural vibration and flutter behavior, since it only accounts for a more uniform distribution of the mass and stiffness without changing their overall values. The flutter results show the expected increase as input Mach number and altitude are changed from $M = 0.60$ at 5000 ft to $M = 0.87$ at 30,000 ft, but show very little differences between the three models for the same respective flight condition. These small existing differences can possibly be attributed to a slight deterioration in the quality of the aspect ratios of the panels for the 7 and the 21 bay wings from those of the 14 bay wing, as well as to the way the wing root section is modeled between the three wings.

Medium Aspect Ratio Wing

For all models of the medium aspect ratio wing, the structural weight was assumed to constitute about 25% of the overall weight of the wing, with the other 75% distributed as nonstructural masses at all structural nodal points and MPCs.

Here, the influence of the aerodynamic wing model complexity was evaluated. The number of aerodynamic boxes on the wing was increased from an initially very coarse grid (5 spanwise by 5 chordwise) by increasing the number of spanwise subdivisions to 11 and 22. Then, the number of aerodynamic boxes on the wing was increased from the same coarse initial 5×5 grid by doubling the number of chordwise subdivisions. For most of the cases, the reasonable width-to-length ratio of the aerodynamic boxes was exceeded to determine how forgiving the aerodynamic modeling process is.

The results are presented here in comparison to a more reasonable spanwise and chordwise subdivision of 22×10 (Table 5). Similar to the results for the Rudisill and Bhatia wing model, the flutter speed changed little for all the different types of meshes. Here, as for the Rudisill and Bhatia wing, the models with a lower number of chordwise boxes showed slightly lower flutter speeds, while increasing the number of spanwise boxes raised the flutter speeds.

Then, the use of MPCs was evaluated. These MPCs add nonstructural points rigidly splined to existing structural points for two purposes: 1) to attach masses for better overall mass distribution and 2) to add points to which the aerodynamic loads can be surface splined for better aerodynamic load distribution (Fig. 5). They had been used in all above-mentioned computations for the medium aspect ratio wing. Here, the additional aerodynamic force transfer points and mass points

were omitted on a model with an aerodynamic mesh of 22 × 10. Only out-of-plane displacements were included in the analyses.

It seems from the results in Table 6 that the use of MPCs for better distribution of the nonstructural mass away from just the structural wing box has the effect of lowering the natural frequencies slightly. Also, larger rotational moments are produced due to this offset. This effect, together with that of the MPCs used for splining the aerodynamic forces to a larger area than just the structural wing box, dropped the flutter speed for the lowest frequency flutter mode by about 12%. It has to be pointed out that additional flutter modes existed for the wing without MPCs (a low damping mode with lower flutter speed at higher frequency and a divergence mode slightly above the speed of the lowest frequency flutter mode), and for the wing with only mass MPCs (a hump mode with lower flutter speed at the same frequency as the low damping mode of the no-MPC wing model). Thus, the use of MPCs seems indicated for a realistic flutter analysis, at least for wings that have the structural wing box located such that elastic axis and c.m. are in close proximity.

Finally, various overlaps were investigated for the splining of the aerodynamic coefficients to the structural grid points. The inboard (straight) and outboard (tapered) sections of the wing were treated as separate aerodynamic surfaces. All previously mentioned results were obtained with the aerodynamic coefficients for each surface splined only to the respective underlying structure. Now, the coefficients from each surface were splined to the underlying structure plus to additional rows of structural nodal points on the structure underlying the respective other surface, resulting in an overlapping splining scheme.

The results (Table 7) show a slight decrease in flutter speed as the aerodynamic forces are distributed more and more over the adjoining structural sections. As the inboard section is covered and only an increase in the distribution over the outboard section continues, the flutter speed shows a slight increase.

Table 7 Varying overlap of splines on medium aspect ratio wing model

Nodal rows of splining overlap				
None	One	Two	Three	Four
Flutter speed, in./s				
20,240	20,202	20,173	20,187	20,195

Table 8 Varying spar number on low aspect ratio wing model

Internal spars	
5	10
Natural frequency, Hz	
5.23 B	4.67 B
21.18 B/T	18.29 B/T
24.79 B/T	24.63 B/T
37.36 I	29.56 I
37.78 B/T	37.81 B/T
57.67 B/T	45.99 B/T
Flutter speed, in./s	
25,367	24,948

B = bending, T = torsion, I = in-plane.

Low Aspect Ratio Wing

For the low aspect ratio wing (Figs. 6a and 6b), nonstructural mass in the amount of 2400 lb was distributed over all nodal points, and a mass of 200 lb for a wingtip store with launcher was distributed over the wingtip points. No MPCs were used, since the wing box covers a large part of the projected wing area. An aerodynamic mesh of 15 × 15 boxes was chosen.

For this wing, the influence of structural complexity in chordwise direction was evaluated. Starting with a reasonable model for the wing box using five internal spars, the wing was then subdivided by adding five more spars while keeping the total weight constant. The influence of a more evenly distributed stiffness and mass arrangement was thus evaluated. Results for the subsonic case with $M = 0.85$ are presented in Table 8.

The results suggest that distributing mass and stiffness more evenly in chordwise direction reduces the natural frequencies, especially in the two lowest modes while also lowering the flutter speed slightly. Thus, the coarser model in chordwise direction seems to be nonconservative.

Also, the influence of input Mach number on flutter speed was evaluated as the aerodynamic coefficients were calculated for subsonic ($M = 0.5$–0.85), transonic ($M = 0.85$–1.2), and supersonic speeds ($M = 1.2$–1.5). It has to be pointed out that the aerodynamic modules in ASTROS compute aerodynamic coefficients only by linear theory and, thus, do not account for the nonlinearities of shock development in the transonic regime.

The results showed (Table 9) that, with an increase in input Mach number, the flutter speed decreased in the subsonic regime and increased in the supersonic regime. Reasonably converged (linear) results were obtainable up to $M = 0.92$ and above $M = 1.2$. At $M = 0.95$ and 1.15, a lower speed hump mode emerged in addition to the regular flutter mode. For $M = 1.1$, no converged results could be obtained.

Discussions and Recommendations

The flutter analysis portion of ASTROS was used for investigations of fully built-up finite element wing models to determine the influences of structural and aerodynamic modeling on flutter analysis. Thus, the behavior of the analyses modules in the code was investigated with the long-range goal of gaining a better understanding of the optimization process with aeroelastic constraints.

Table 9 Varying input Mach number on low aspect ratio wing model

Initial speed selection, M, subsonic:	0.50	0.75	0.85	0.90	0.92	0.95
Flutter speed, in./s	31,440	28,716	25,367	22,709	21,168	18,400 + hump
Initial speed selection, M, supersonic:	1.10		1.15		1.20	1.50
Flutter speed, in./s	No convergence		23,616 + hump		25,667 + hump	34,723

Several trends could be observed during the course of the modeling, the free vibration analyses, and the flutter analyses, even though it is understood that until many more cases have been evaluated any set of analyses has to be regarded as more or less wing type and model specific.

A quick initial evaluation of a preliminary design with a reasonably coarse grid for both the structure and the aerodynamics will result in natural frequencies and modes that are close to those from a more detailed model, whereas this evaluation will also result in flutter speeds that are, for the most part, conservative. Here, the chordwise distribution needs more attention than the spanwise one in the structural modeling, while, for the aerodynamic modeling, the opposite seems indicated. In general, however, a good start is obtained for a conventional redesign process as well as for optimization.

The selection of the correct finite elements for modeling the structure is rather critical since, e.g., choosing membrane instead of shear elements can, in some cases, result in nonconservative flutter speeds as well as overly low weights in optimization.

The use of mass MPCs is advised for a more realistic mass distribution, and that of splining MPCs for a better aerodynamic force distribution. Omission of MPCs can result in increased flutter speeds and can be nonconservative. Using overlaps in the splining of multiple spanwise aerodynamic surfaces seems to be mostly conservative and to have little influence on the flutter speed.

An issue of interest has resurfaced during the course of these analyses. In most cases, when a model was evaluated for flutter at subsonic speeds, a supersonic flutter speed resulted. The opposite also can occur: a subsonic flutter speed resulting from a supersonic analysis. This problem, the two-way crossing over the transonic regime, is presently being addressed in a parametric study.

Finally, most of the results presented here addressed the influence of structural and aerodynamic modeling on flutter and normal modes analysis only. However, some results have been obtained on how various parameters and modeling errors affect the final minimum weight design in optimization with a flutter constraint.[14] A detailed study in this area is continuing using again ASTROS, this time, however, in the design mode with a flutter constraint.

Acknowledgments

The authors would like to acknowledge Victoria Tischler and Mark French of the Flight Dynamics Laboratory, Wright Laboratories, Wright-Patterson AFB, Ohio, for helpful technical discussions and computational support. Also to be mentioned are the students of a graduate course on aeroelasticity at the University of Oklahoma, Norman, Oklahoma, and especially Gregory Hughes of Manufacture Engineering Units, Tinker AFB, Oklahoma, for their contributions.

References

[1]Johnson, E. H., and Venkayya, V. B., "Automated Structural Optimization System (ASTROS), Vol. I: Theoretical Manual," Air Force Wright Aeronautical Labs., AFWAL-TR-88-3028/I, Wright-Patterson AFB, OH, Dec. 1988.

[2]Neill, D. J., Johnson, E. H., and Herendeen, D. L., "Automated Structural Optimization System (ASTROS), Vol. II: User's Manual," Air Force Wright Aeronautical Labs., AFWAL-TR-88-3028/II, Wright-Patterson AFB, OH, April 1988.

[3]Johnson, E. H., and Neill, D. J., "Automated Structural Optimization System (ASTROS), Vol. III: Applications Manual," Air Force Wright Aeronautical Labs., AFWAL-TR-88-3028/III, Wright-Patterson AFB, OH, Dec. 1988.

[4]Rodden, W. P. (ed.), *MSC/NASTRAN Handbook for Aeroelastic Analysis*, The MacNeal-Schwendler Corp., Los Angeles, CA, 1987.

[5]Taylor, R. F., Miller, K. L., and Brockman, R. A., "A Procedure for Flutter Analysis of FASTOP-3 Compatible Mathematical Models," Air Force Wright Aeronautical Labs., AFWAL-TR-81-3063, Wright-Patterson AFB, OH, Aug. 1981.

[6]Garner, G., and French, M., "A Comparison of Supersonic Flutter Predictions for a Straight Wing," Air Force Wright Aeronautical Labs., AFWAL-TM-88-176-FIBR, Wright-Patterson AFB, OH, May 1988.

[7]Pendleton, E., French, M., and Noll, T., "A Comparison of Flutter Analyses for a 45° Swept Model," AIAA Paper 87-2886, Sept. 1987.

[8]Rudisill, C. S., and Bhatia, K. G., "Optimization of Complex Structures to Satisfy Flutter Requirements," *AIAA Journal*, Vol. 9, No. 8, 1971, pp. 1487–1491.

[9]Rudisill, C. S., and Bhatia, K. G., "Second Derivatives of the Flutter Velocity and the Optimization of Aircraft Structures," *AIAA Journal*, Vol. 10, No. 12, 1972, pp. 1569–1572.

[10]McIntosh, S. C., Jr., and Ashley, H., "On the Optimization of Discrete Structures with Aeroelastic Constraints," *Computers and Structures*, Vol. 8, Nos. 3/4, 1978, pp. 411–419.

[11]Segenreich, S. A., and McIntosh, S. C., "Weight Minimization of Structures for Fixed Flutter Speed Via an Optimality Criterion," AIAA Paper 75-0779, May 1975.

[12]Eastep, F. E., private communication, Univ. of Dayton, Dayton, OH.

[13]Striz, A. G., "Realistic Structural and Aerodynamic Wing Models for Flutter Analysis and Structural Optimization," Univ. of Oklahoma, OU-AME-TR-90-110, Norman, OK, Jan. 1990.

[14]Striz, A. G., and Venkayya, V. B., "Influence of Structural and Aerodynamic Modeling on Optimization with Flutter Constraint," USAF/NASA Symposium on Recent Advances in Multidisciplinary Analysis and Optimization, San Francisco, CA, Sept. 1990.